

Innovative Diffusion Driven Desalination Process

James F. Klausner, Mohamed Darwish, and Renwei Mei
University of Florida
Department of Mechanical and Aerospace Engineering
Gainesville, Florida 32611

Abstract

An innovative diffusion driven desalination (DDD) process is presented, and its performance based on thermodynamic considerations is thoroughly explored. The desalination is driven by water vapor saturating dry air flowing through a diffusion tower. Liquid water is condensed out of the air/vapor mixture in a direct contact condenser. The desalination process is suitable for operation at low temperatures and may be driven by waste heat with low thermodynamic availability. It is demonstrated that the DDD process can yield a fresh water production efficiency of 8% with an energy consumption of 0.05 kWh per kilogram of fresh water production based on a feed water temperature of only 60° C. An example is discussed in which the DDD process utilizes waste heat from a 100 MW steam power plant to produce 18 million gallons of fresh water per day. The energy consumption for the DDD process is comparable to that for conventional flash evaporation and reverse osmosis processes.

1.0 Introduction

The continuous rise in the world population and the expansion of industrial facilities around the globe has placed a growing demand on the fresh water supply from natural resources (rivers, fresh water lakes, underground aquifers, and brackish wells). These resources have been steadily on the decline since the early 1950's. Therefore the need for new fresh water resources to balance the growing consumption rate has been a

serious concern facing governments and world organizations for the past 50 years. The fact that 96% of the earth's surface is covered with saline water has been a substantial catalyst for developing water desalination technologies. Today there are more than 7500 desalination plants in operation worldwide, and about two thirds of those are operating in the Middle East. Saudi Arabia operates the largest desalination plant, with a capacity of 128 MGD. The United States accounts for about 12% of the world's desalination capacity, with the majority of production in Florida and the Caribbean [1].

Desalination involves any process in which dissolved minerals are removed from saline or brackish water. Technologies developed for desalination applications include distillation, reverse osmosis, electro-dialysis, and vacuum freezing. Distillation and reverse osmosis are the most commercially prominent. Distillation technologies include Multiple Effect Distillation (MED) and Multi-Stage Flashing (MSF), both of which operate by evaporating saline water at atmospheric or reduced pressure and condensing the vapor to produce fresh potable water. Reverse Osmosis (RO) operates on a filtering principle. High pressure pumps force the saline water through nanofilter membranes allowing fresh water to pass while filtering out the dissolved minerals. Although distillation and reverse osmosis technologies currently provide the most cost effective means for desalination, their drawback is that they are very energy intensive, and whether or not they remain cost effective strongly depends on energy prices and energy supply.

A desalination technology that has drawn interest over the past two decades is referred to as Humidification Dehumidification (HDH). This processes operates on the principle of mass diffusion and utilizes dry air to evaporate saline water, thus humidifying the air. Fresh water is produced by condensing out the water vapor, which

results in dehumidification of the air. A significant advantage of this type of technology is that it provides a means for low pressure, low temperature desalination and can potentially be very energy efficient. Bourouni et al., Al-Hallaj et al., and Assouad et al. [2-4] respectively reported the operation of HDH units in Tunisia, Jordan, and Egypt. Another type of desalination technology that makes use water evaporating into an air stream is the Carrier-Gas Process (CGP) reported by Larson et al. [5]. An economic analysis was provided to suggest that such a technology has potential economic advantages compared with conventional MED, MSF, and RO technologies.

This work describes a new Diffusion Driven Desalination (DDD) process that demonstrates competitive thermal efficiency advantages with conventional desalination technologies at large production rates. The DDD process is in some ways similar to the HDH and CGP processes in that the mass diffusion of water molecules into dry air is the driving mechanism to evaporate saline water. In addition, the DDD process makes use of the naturally occurring thermal energy storage in large bodies of water, where desalination is most likely to be applicable. Because the desalination is accomplished at relatively low temperatures, inexpensive materials may be used for constructing a processing facility, and waste heat may be utilized to drive the desalination process. A complete thermodynamic analysis of the DDD process has been explored and it is demonstrated that the process has substantial potential for cost reduction when compared with conventional desalination technologies. Its potential benefit to the electric utility industry is discussed.

2.0 The Diffusion Driven Desalination Process

A simplified schematic diagram of the DDD process and system are shown in Figure 1. The process is described here. A main feed pump (a) draws water from a large body of seawater. The suction for the pump draws water near the surface in order to take advantage of the fact that large bodies of water absorb solar radiation, and due to thermal stratification, the warmer water is in the vicinity of the surface, while cooler water resides at larger depths beneath the surface. The surface water is pumped through the main feed water heater (b). The amount of heat required depends on the main feed water mass flow rate and desired production rate. The output temperature from the heater is relatively low, and therefore the required heat input can be provided by a variety of sources, depending on the available resources. It is envisioned that heat can be provided from low pressure condensing steam in the main condenser of a steam driven power plant, waste heat from a combustion engine, solar heating, or from a direct fossil fuel fired furnace. After the feed water is heated in the main heater, it is sprayed into the top of the diffusion tower (c). The diffusion tower is the most important piece of equipment in the process, and the degree to which an operational DDD process follows theoretically predicted trends depends on an appropriately designed diffusion tower. On the bottom of the diffusion tower, low humidity air is pumped in using a forced draft blower (d). The water falls concurrently to the airflow through the diffusion tower by the action of gravity. The diffusion tower is packed with very high surface area packing material, as would be found in an air-stripping tower. As water flows through the diffusion tower, a thin film of water forms over the packing material and contacts the air flowing upward through the tower. As dictated by Fick's law and the conservation of mass, momentum, and energy,

liquid water will evaporate and diffuse into the air, while air will diffuse into the water, due to concentration gradients. The diffusion tower should be designed such that the air/vapor mixture leaving the diffusion tower should be fully saturated. The purpose of heating the water prior to entering the diffusion tower is that the rate of diffusion and the exit humidity ratio increase with increasing temperature, thus yielding greater production. The water not evaporated in the diffusion tower, will be collected at the bottom and removed with a brine pump (e). The brine will either be discharged or sent through a regenerative heater (i). When the brine temperature exceeds 30° C, it will be sent to the regenerative heater, otherwise it will be discharged. With appropriate maintenance it is not expected that scaling of the diffusion tower will pose a significant problem since the brine will wash away residual minerals left behind by the evaporated water.

The air entering the diffusion tower will be dried in the direct contact condenser (g). The saturated air/vapor mixture leaving the diffusion tower is drawn into the direct contact condenser with a forced draft blower (f), where the water vapor is condensed into fresh liquid water that is collected in the sump of the condenser. Another very important component of the DDD process is the condenser. The difficulty that arises is that film condensation heat transfer is tremendously degraded in the presence of non-condensable gas. The same difficulty was faced in the design and development of condensers for OTEC (Ocean Thermal Energy Conversion) applications. In order to overcome this problem Bharathan et al. [6] describe the use of direct-contact heat exchangers. In their excellent report, they have developed models for simulating the heat transfer and have validated the models with careful experimentation. Bharathan et al. [7] have also been awarded a U.S. Patent for a high efficiency direct contact heat exchanger. For the present

application involving desalination, the warm fresh water discharging the direct contact heat exchanger will be chilled in a conventional shell-and-tube heat exchanger (h) using saline cooling water. The cooling water is drawn from a large depth to take advantage of the thermal stratification in large bodies of water. A portion of the chilled fresh water will be directed back to the direct contact heat exchanger to condense the water vapor from the air/vapor mixture discharging from the diffusion tower. The rest of the fresh water is make-up water. The direct contact condenser approach is best suited for the DDD process.

3.0 Analysis and Results

In order to explore the performance and parametric bounds of the Diffusion Driven Desalination process, a thermodynamic cycle analysis has been performed. In performing the analysis the following assumptions have been made,

1. The process operates at steady-state conditions,
2. There are no energy losses to the environment from the heat and mass transfer equipment,
3. Air and water vapor may be treated as a perfect gas,
4. Changes in kinetic and potential energy are relatively small,
5. The pumping power is neglected in the energy balance (estimating the required pumping power would require significant details regarding the construction of the diffusion tower and heat transfer equipment; these are beyond the scope of the current analysis).

In the analysis, the temperature of the feed water drawn into the main feed pump is fixed at 27° C. It is assumed that a large supply of cool water will be available at a sink temperature, T_L , of 15° C. The condensate in the direct contact condenser will be chilled and a portion of it re-circulated. To avoid providing specifics on the heat transfer equipment, it is assumed that the heat transfer effectiveness in the chiller and condenser is unity, in which case $T_L=T_5=T_7=15^\circ\text{C}$. The temperature of the feed water leaving the main heater is the high temperature in the system, $T_H=T_1$, and is a primary controlling variable for the process. Different performance curves will be shown for a variable T_H/T_L .

The air/vapor mixture leaving the diffusion tower is assumed to be fully saturated (relative humidity of unity), and due to heat transfer limitations, its maximum temperature will be taken to be that of the feed water entering the diffusion tower ($T_4=T_1$).

The main purpose of this analysis is to explore the performance bounds of the DDD process. However, specification of the system operating variables is not arbitrary. Namely there are two constraints that must be satisfied,

1. The brine temperature leaving the diffusion tower must not freeze ($T_2>0^\circ\text{C}$), and
2. The net entropy generation in the diffusion tower must be positive.

These constraints govern the parametric bounds for the diffusion tower operation. While the first constraint is initially obvious, the second constraint is simply a restatement of the second law of thermodynamics for the present adiabatic system (diffusion tower). The control volume formulation of the second law of thermodynamics for an open system is expressed as,

$$\frac{Ds}{Dt} = \frac{\partial}{\partial t} \int_V \rho s dV + \oint_A \rho s \vec{v} \cdot d\vec{A} \geq \oint_A \frac{1}{T} \frac{\dot{Q}}{A} dA, \quad (1)$$

where V denotes the control volume, A is the control surface, and s is the entropy per unit mass. Assuming steady state processing of fresh water, the adiabatic diffusion tower assumption leads to,

$$\dot{s} = \frac{Ds}{Dt} = \oint_A \rho s \vec{v} \cdot d\vec{A} \geq 0, \quad (2)$$

and

$$\dot{s} = m_{l2}s_{l2} + m_a s_{a4} + m_{v4}s_{v4} - m_{l1}s_{l1} - m_a s_{a3} - m_{v3}s_{v3} \quad (3)$$

where m denotes the mass flow rate and the subscripts l, a, and v respectively refer to the liquid, air, and vapor phases. The numerical subscripts denote that the property is evaluated at the state corresponding to the position in the process as shown schematically in Figure 1. Conservation of mass dictates that,

$$\frac{m_{l2}}{m_a} = \frac{m_{l1}}{m_a} - (\omega_4 - \omega_3). \quad (4)$$

The rate of entropy generation in the diffusion tower per rate of air flow, which must be positive, is obtained from rearranging Eq. (3) and combining with Eq. (4) as,

$$\frac{\dot{s}}{m_a} = \left[\frac{m_{l1}}{m_a} - (\omega_4 - \omega_3) \right] s_{l2} + C_{pa} \ln \left(\frac{T_4}{T_3} \right) - R_a \ln \left(\frac{P_{a4}}{P_{a3}} \right) + \omega_4 s_{v4} - \omega_3 s_{v3} - \frac{m_{l1}}{m_a} s_{l1}, \quad (5)$$

where ω is the humidity ratio, C_p is the specific heat, R is the engineering gas constant, and P_a is the partial pressure of air.

The control volume formulation of energy conservation applied to the adiabatic diffusion tower leads to,

$$m_{l1}h_{l1} + m_a h_{a3} + m_{v3}h_{v3} - m_{l2}h_{l2} - m_a h_{a4} - m_{v4}h_{v4} = 0 \quad (6)$$

where h denotes the enthalpy. The enthalpy of the brine exiting the diffusion tower is obtained from Eqs. (6) and (4) as,

$$h_{l2}(T_2) = \frac{\frac{m_{l1}}{m_a} h_{l1} - C_{pa}(T_4 - T_3) + \omega_3 h_{v3} - \omega_4 h_{v4}}{\frac{m_{l1}}{m_a} - (\omega_4 - \omega_3)}, \quad (7)$$

and the brine temperature (T_2) is evaluated from the enthalpy. The ratio of the feed water to air flow through the diffusion tower, $\frac{m_{l1}}{m_a}$, is another controlling variable in the analysis. For all computations the feed water flow rate will be fixed at 1 kg/s while the air flow rate will be varied.

The humidity ratio entering the diffusion tower, ω_3 , is determined by recognizing that it is the same as the humidity ratio exiting the condenser, where T_7 is 15 °C. Prior to entering the diffusion tower, the air/vapor mixture is convectively heated by the ambient as it is pumped back to the diffusion tower. This may be achieved by placing fins on the return line to the diffusion tower. Taking the ambient temperature to be 25 °C, it follows that $T_3=25$ °C and $\omega_3=\omega_7$.

The first case considered is where there is no heating in the main heater. The desalination process is entirely driven by the difference in temperature of the feed water drawn at shallow depths and the cooling water drawn at more substantial depth. In this case, $T_H/T_L=1.04$. Figure 2 shows the rate of entropy generation within the diffusion tower and the brine temperature exiting the diffusion tower for a locus of possible operating conditions. Here it is observed that the second law of thermodynamics is satisfied for the entire parametric range considered. At the highest air to feed water flow ratio, more fresh water production is possible, but there is a lower limit beyond which the

exit brine will freeze. Figure 3 shows the brine temperature (T_2) exiting the diffusion tower as a function of the exit air temperature from the diffusion tower (T_4) for the same locus of operating conditions as in Figure 2. It is advantageous to have a high air temperature leaving the diffusion tower so that the humidity ratio and fresh water production rate are as high as possible. For this case the exit air temperature is primarily constrained by the inlet feed water temperature (T_1). Due to heat transfer considerations it would be impractical to design the diffusion tower such that T_4 exceeds T_1 . Thus in this analysis, the exiting air temperature from the diffusion tower does not exceed the inlet feed water temperature. Figure 4 shows the ratio of fresh water production rate to the inlet feed water rate as a function of the exit air temperature for different air to feed water flow ratios. Clearly, the production rate increases with increasing exit air temperature and increasing air to feed water flow ratios. However, both these parameters are constrained, and for the case of no heating of the feed water ($T_H/T_L=1.04$), the maximum fresh water production efficiency (m_{fw}/m_{l1}) is approximately 0.035.

The next cases considered are where the diffusion tower inlet water temperatures are 60°C and 80°C which correspond to $T_H/T_L=1.156$ and 1.23 , respectively. Figures 5 and 6 show the rate of entropy generation in the diffusion tower for $T_H/T_L=1.156$ and 1.23 , respectively. Again the second law of thermodynamics is satisfied for the entire parametric range considered. The entropy generation tends to be lower for lower air to feed water flow ratios and higher exit brine temperatures. At higher air to feed water flow ratios, the constraint is that the brine does not freeze. Figure 7 shows the range of possible exit brine temperatures and exit air temperatures for different air to feed water flow ratios when the diffusion tower inlet water temperature is 60°C ($T_H/T_L=1.156$).

Figure 8 shows the range of temperatures when the diffusion tower inlet water temperature is 80°C ($T_H/T_L=1.23$). The maximum fresh water production will occur with as high an exit air temperature as possible. In order to satisfy an energy balance on the diffusion tower, the exit brine temperature decreases with increasing exit air temperature. In contrast to the case with no heating, the exit air temperature is primarily constrained by the fact that the brine cannot freeze, especially at higher air to feed water flow ratios. At very low air to feed water flow ratios and $T_L=60^{\circ}$ and 80°C , the exit air temperature is constrained by the inlet water temperature.

For respective diffusion tower inlet water temperatures of 60°C and 80°C , Figures 9 and 10 show the ratio of fresh water production to the inlet feed water flow rate as a function of the exit air temperature for different air to feed water flow ratios. It is observed that the fresh water production efficiency increases with increasing exit air temperature and increasing air to feed water flow ratio. The maximum fresh water production efficiency for $T_i=60^{\circ}\text{C}$ is approximately 0.08, while that for $T_i=80^{\circ}\text{C}$ is approximately 0.11. Therefore, one advantage of increasing the diffusion tower inlet water temperature is that the fresh water production efficiency increases.

For respective diffusion tower inlet water temperatures of 60°C and 80°C , Figures 11 and 12 show the energy consumed per unit of fresh water production as a function of exit air temperature for different air to feed water flow ratios over the entire parameter space considered. Although, details of the low energy consumption regime are difficult to discern, it is interesting to observe that increasing both the exit temperature and the air flow results in a reduced rate of energy consumption. In order to explore the lower energy consumption regime Figures 13 and 14 have been prepared for diffusion

tower inlet water temperatures of 60° C and 80° C, respectively. For $T_1=60^\circ$ C the lower limit on energy consumed per unit of fresh water production is about 0.06 kWh/kg_{fw} while that for $T_1=80^\circ$ C is approximately 0.05 kWh/kg_{fw}. In this analysis the energy consumption due to pumping is neglected, and the current results suggest that the energy consumption is lower with higher air to feed water flow ratios. However, with higher air flow, the pumping power required will increase as well. Therefore, it is expected that in actual practice there is some minimum energy consumption associated with a specific air to feed water flow ratio that is less than the maximum flow. The inclusion of the pumping power in the overall analysis is the subject of a future investigation.

It is also of interest to compare the fresh water production and energy consumption between the cases of $T_1=60^\circ$ and 80° C. There is only marginal improvement in the fresh water production and energy consumption when increasing T_H from 60 to 80 ° C. This demonstrates that the DDD process is best suited for applications where the waste heat driving the process has low thermodynamic availability, as will be described in the next section.

4.0 Applications

The energy consumption for the DDD process is comparable to that for flash distillation and reverse osmosis. The major advantage of the DDD process is that it can operate at low temperatures so that it requires an energy input with low thermodynamic availability. This is important because the process can be driven by waste heat that would otherwise not be suitable for doing useful work or driving some other distillation process (such as flash distillation). A very interesting application for the DDD process is

to operate in conjunction with an existing process that produces large amounts of waste heat and is located in the vicinity of an ocean or sea. One such potential benefactor of the DDD process is the electric utility industry. Conventional steam driven power plants dump a considerable amount of energy to the environment via cooling water that is used to condense low pressure steam within the main condenser. Typically this cooling water is either discharged back to its original source or it is sent to a cooling tower, where the thermal energy is discharged to the atmosphere. Instead of dumping the thermal energy to the environment, the DDD process provides a means for putting the discarded thermal energy to work to produce fresh water. Of course this application is limited to power producing facilities sited along the coastline. However, this should not be a significant limitation. Bullard and Klausner [8] studied the geographical distribution of fossil fired power plants built in the United States from 1970 to 1984. In their study they found that the two most significant attributes for siting a new fossil fired plant in a given geographical region are 1) proximity to a large body of water and 2) proximity to a large population base. The demographic make-up of the United States as well as other industrialized nations is such that major population centers reside along the coastline. Thus, the DDD process appears to be well suited for the power generation infrastructure in the United States.

As an example, consider that a 100 MW steam driven power plant operating with 2" Hg vacuum in the main condenser would have approximately 140 MW of energy at 93° C available from low pressure condensing steam [9]. If retrofitted with a DDD plant, there is potential to produce as much as 18 million gallons of fresh water over a 24 hour period, assuming the DDD process energy consumption to be 0.05 kWh/kg_{fw}. The low

temperature operation of the DDD process is economically advantageous in that inexpensive materials may be used to construct a facility. Since the energy required to drive the DDD process would be free to an electrical utility, it is anticipated that the capital investment required to fabricate a DDD plant could be readily recovered by selling fresh water to local industry and municipalities.

Another point worth mentioning is that although there exists some optimum air to feed water flow ratio that will minimize the energy consumption, this may not be the most economical operating condition when the DDD process is driven by waste heat. The reason is that a higher air flow rate requires more pumping power, which must be supplied to forced draft fans via electricity. Since electricity is a valuable commodity it may be more economical to operate with a higher exit air temperature and a lower air to feed water flow ratio (lower electricity consumption) since the thermal energy driving the DDD process is waste heat that would otherwise be discarded. An economic analysis, which is not considered here, is required to identify the optimum operating conditions based on cost considerations.

5.0 Conclusions

An innovative diffusion driven desalination process has been presented that has the main advantage that it may be driven by waste heat with very low thermodynamic availability. Good performance of the process is realized with an inlet feed water temperature as low as 60° C. The desalination process may also be driven without any heating in applications where there is a temperature gradient between the surface water, which will be drawn in as feed, and the cooling water found at lower depths. It is

envisioned that an excellent application is to place a diffusion driven desalination plant on site at a steam driven electric generating plant, and the waste heat from condensing low pressure steam may be used to drive the desalination process. The potential for producing large quantities of inexpensive fresh water greatly favors further exploration of integrating the DDD process with a steam driven electric generating facility.

References

[1] *Seawater Desalination in California*, 1999, a report by the California Coastal Commission.

[2] Bourouni, K., M. Chaibi, M.T., and Tadrist, L., 2001, "Water desalination by humidification and dehumidification of air: State of the art," *Desalination*, Vol. 137, Issues 1-3, pp. 167-176.

[3] Al-Hallaj, S., Farid, M.M., and Tamimi, A.R., 1998, "Solar desalination with a humidification-dehumidification cycle: performance of the unit," *Desalination*, Vol. 120, Issue 3, pp. 273-280.

[4] Assouad, Y., and Lavan, Z., 1988, "Solar desalination with latent heat recovery," *Journal of Solar Energy Engineering*, Vol. 110, Issue 1, pp. 14-16.

[5] Larson, R.L., Albers, W., Beckman, J., and Freeman, S., 1989, "The carrier-gas process – a new desalination and concentration technology," *Desalination*, Vol. 73, pp. 119-137.

[6] Bharathan, D., Parsons, B.K., and Althof, J.A., 1988, "Direct-Contact Condensers for Open-Cycle OTEC Applications," *National Renewable Energy Laboratory Report SERI/TP-252-3108* for DOE Contract No. DE-AC02-83CH10093.

- [7] Bharathan, D., Parent, A., and Hassani, A. V., 1999, "Method and Apparatus for High-Efficiency Direct Contact Condensation," U.S. Patent 5,925,291.
- [8] Bullard, C.W. and Klausner, J.F., 1987, "Empirical Analysis of Power Plant Siting," *Energy Systems and Policy*, Vol. 11, pp. 103-120.
- [9] El-Wakil, M.M., 1984, *Power Plant Technology*, McGraw-Hill, New York, p. 228.

Nomenclature

A	control surface area (m^2)
C_{pa}	specific heat of air (kJ/kg)
h	enthalpy (kJ/kg)
h_{fg}	latent heat of vaporization (kJ/kg)
m_{l1}	feed water mass flow rate (kg/s)
m_a	air mass flow rate (kg/s)
P_a	partial pressure of air (kPa)
R_a	engineering gas constant for air (kJ/kg-K)
\dot{s}	entropy generation rate in the diffusion tower (kW/K)
T	temperature ($^{\circ}\text{C}$ or $^{\circ}\text{K}$)
V	control volume (m^3)
ω	humidity ratio

Subscripts

a	air
fw	fresh water
l	water in liquid phase
v	water in vapor phase

List of Figures

Figure 1 Flow diagram for diffusion driven desalination process.

Figure 2 Rate of entropy generation in the diffusion tower for $T_H=27^\circ\text{C}$.

Figure 3 Variation of exit brine temperature with exit air temperature for $T_H=27^\circ\text{C}$.

Figure 4 Fresh water production efficiency for $T_H=27^\circ\text{C}$.

Figure 5 Rate of entropy generation in the diffusion tower for $T_H=60^\circ\text{C}$.

Figure 6 Rate of entropy generation in the diffusion tower for $T_H=80^\circ\text{C}$.

Figure 7 Variation of exit brine temperature with exit air temperature for $T_H=60^\circ\text{C}$.

Figure 8 Variation of exit brine temperature with exit air temperature for $T_H=80^\circ\text{C}$.

Figure 9 Fresh water production efficiency for $T_H=60^\circ\text{C}$.

Figure 10 Fresh water production efficiency for $T_H=80^\circ\text{C}$.

Figure 11 Rate of energy consumption for $T_H=60^\circ\text{C}$.

Figure 12 Rate of energy consumption for $T_H=80^\circ\text{C}$.

Figure 13 Rate of energy consumption on magnified scale for $T_H=60^\circ\text{C}$.

Figure 14 Rate of energy consumption on magnified scale for $T_H=80^\circ\text{C}$.

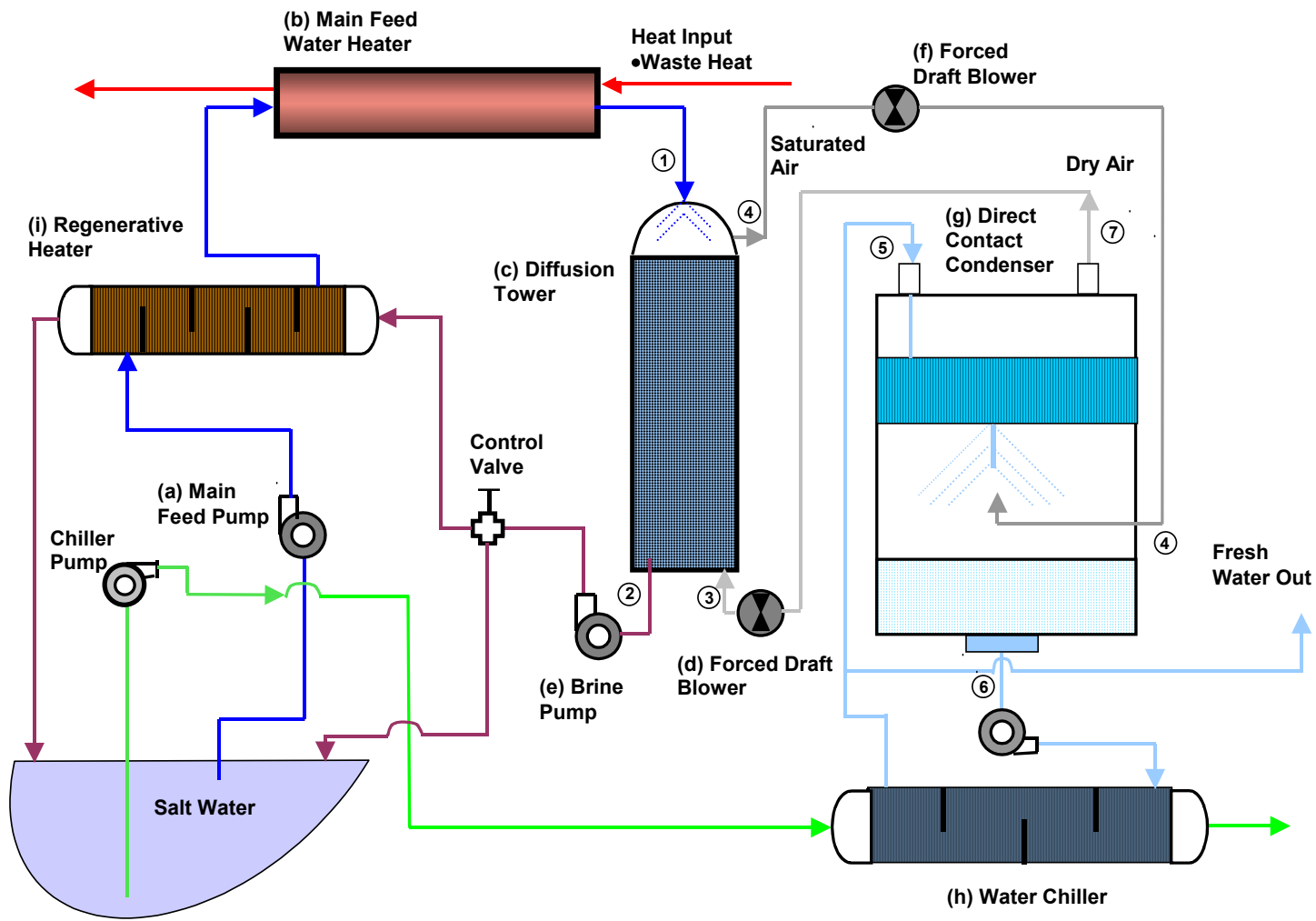


Figure 1 Flow diagram for diffusion driven desalination process.

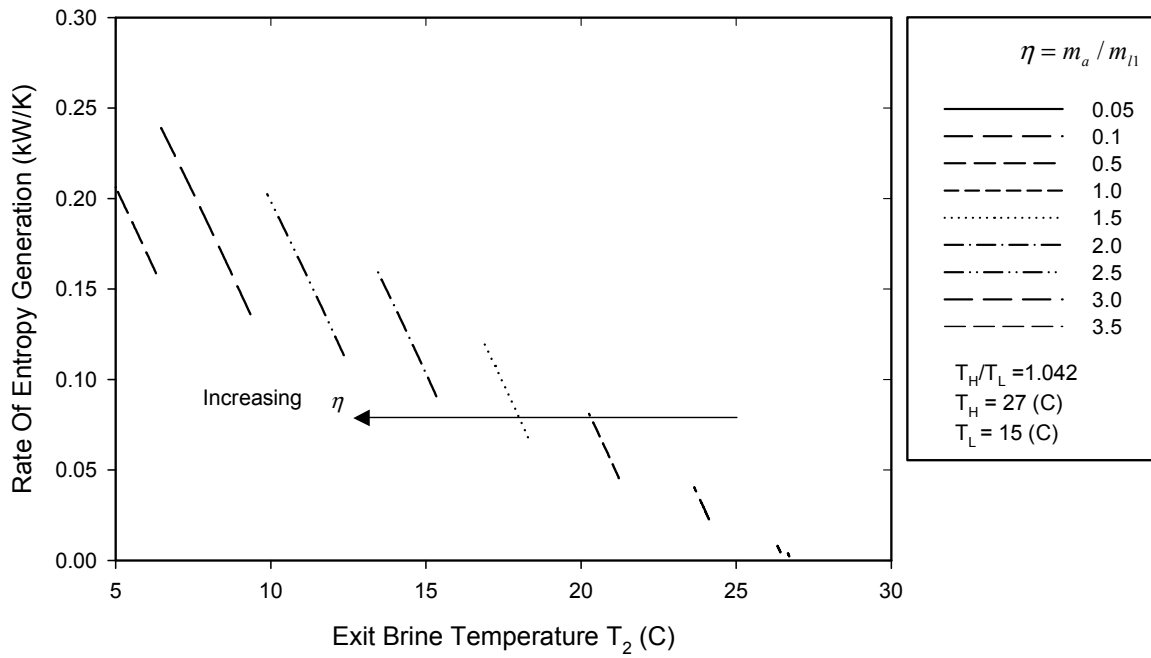


Figure 2 Rate of entropy generation in the diffusion tower for $T_H=27^\circ\text{C}$.

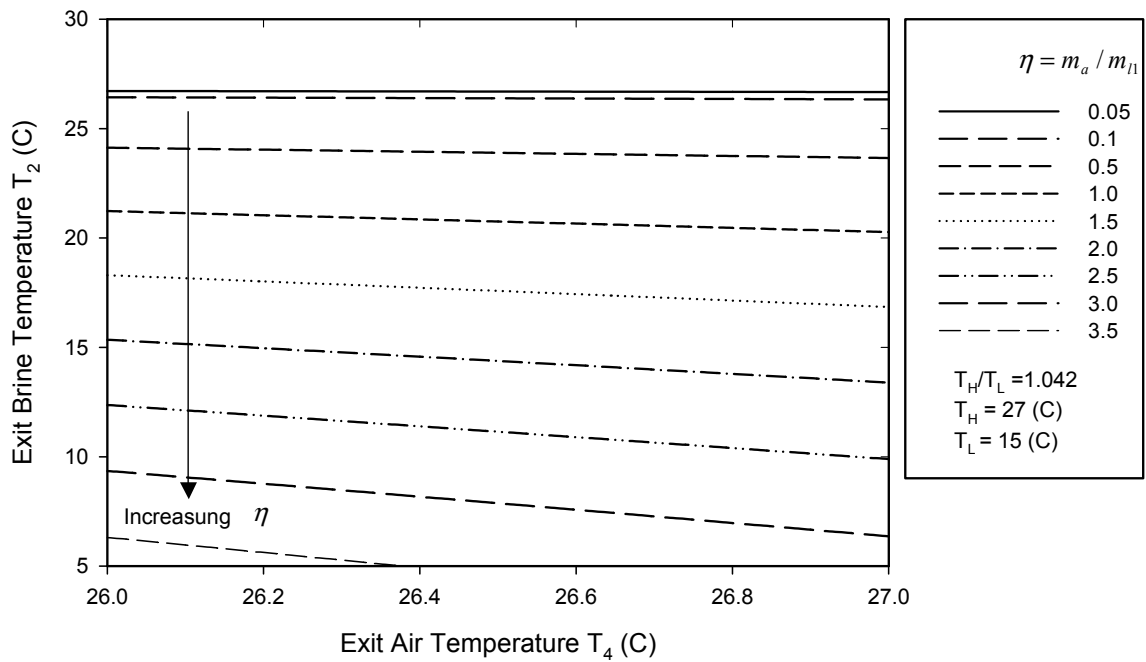


Figure 3 Variation of exit brine temperature with exit air temperature for $T_H=27^\circ\text{C}$.

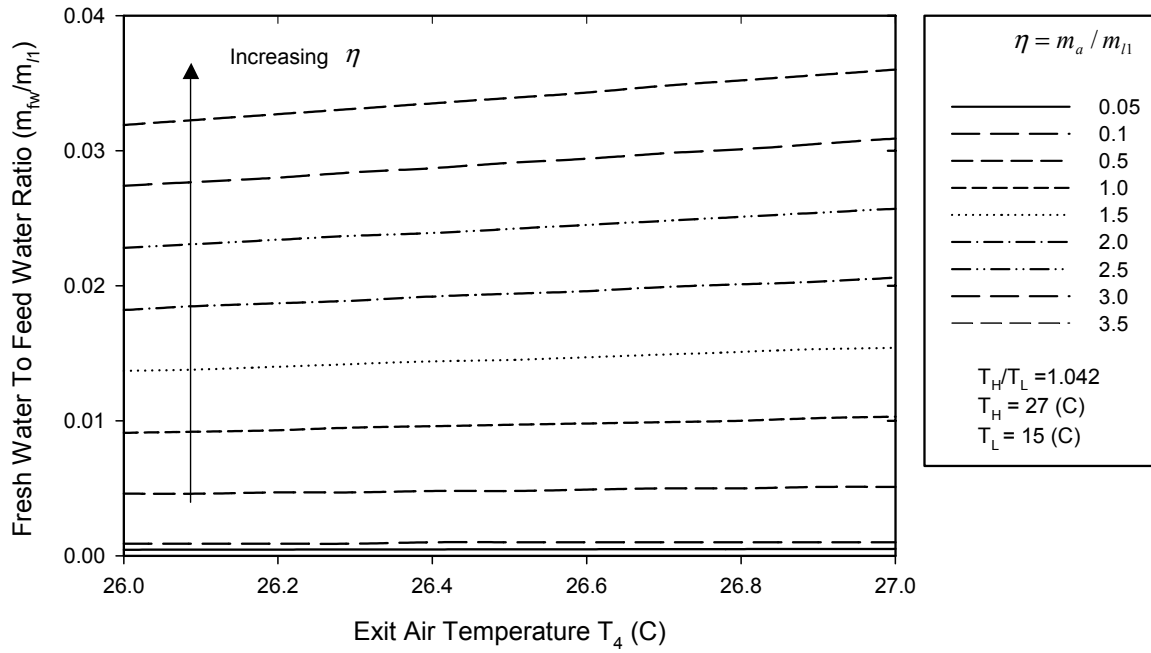


Figure 4 Fresh water production efficiency for $T_H=27^\circ \text{ C}$.

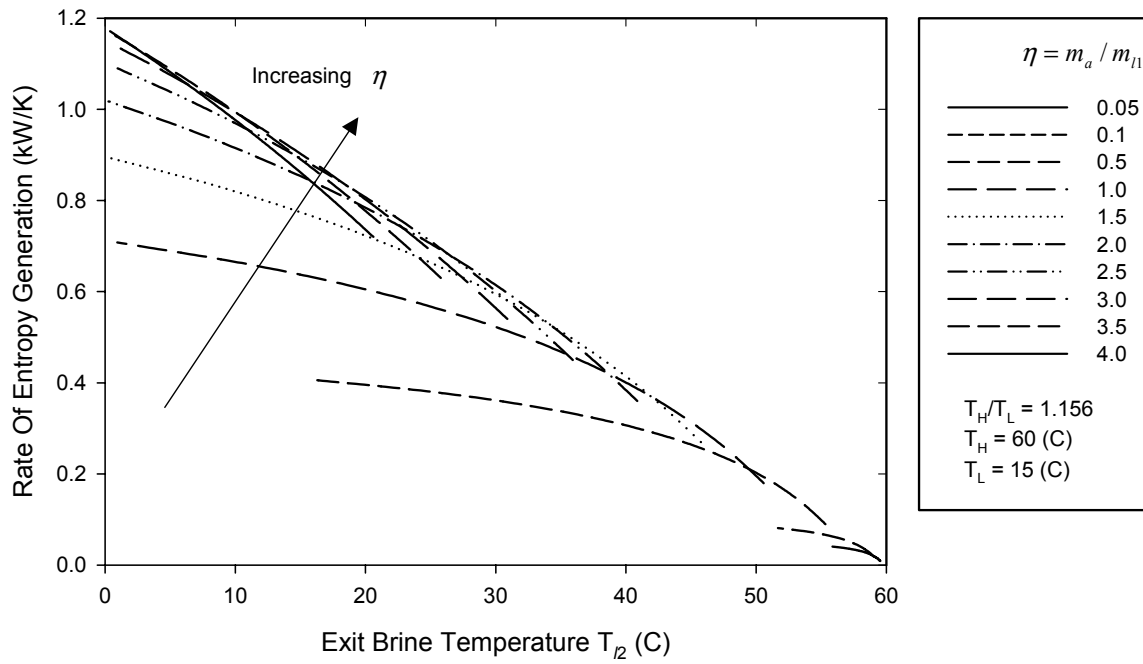


Figure 5 Rate of entropy generation in the diffusion tower for $T_H=60^\circ$ C.

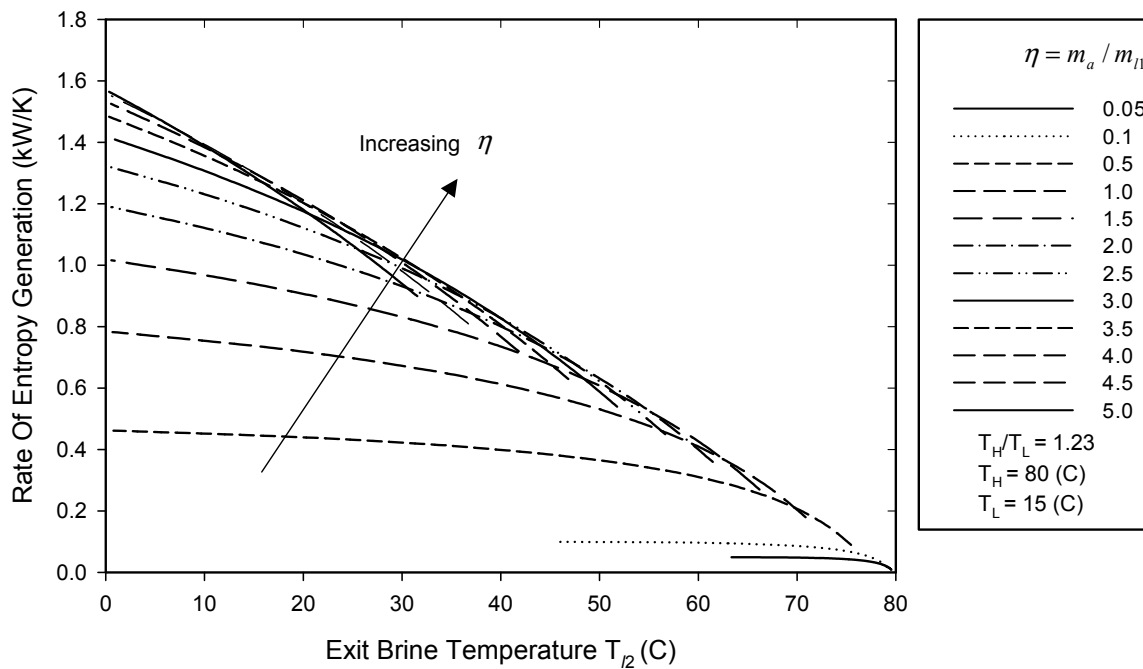


Figure 6 Rate of entropy generation in the diffusion tower for $T_H=80^\circ$ C.

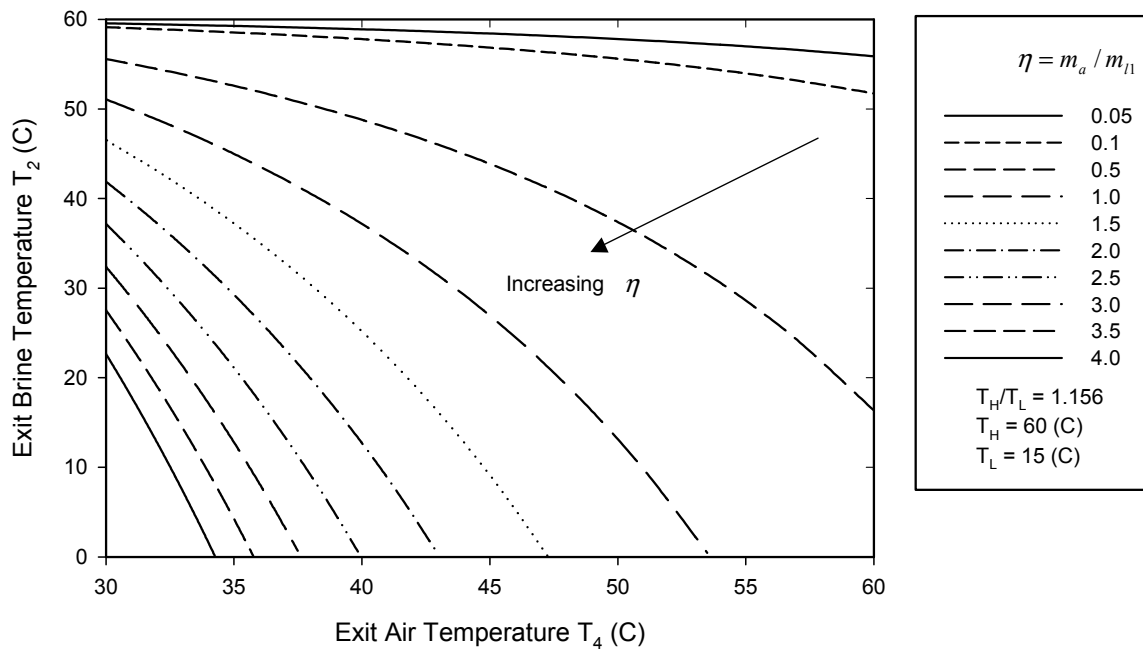


Figure 7 Variation of exit brine temperature with exit air temperature for $T_H = 60^\circ \text{C}$.

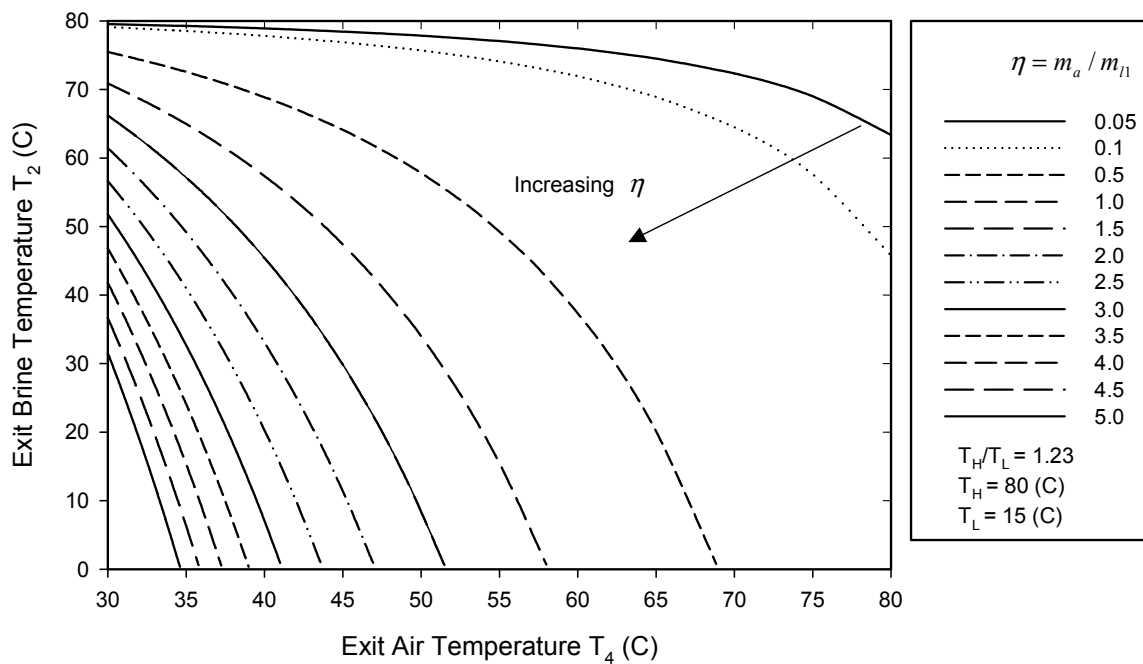


Figure 8 Variation of exit brine temperature with exit air temperature for $T_H = 80^\circ \text{C}$.

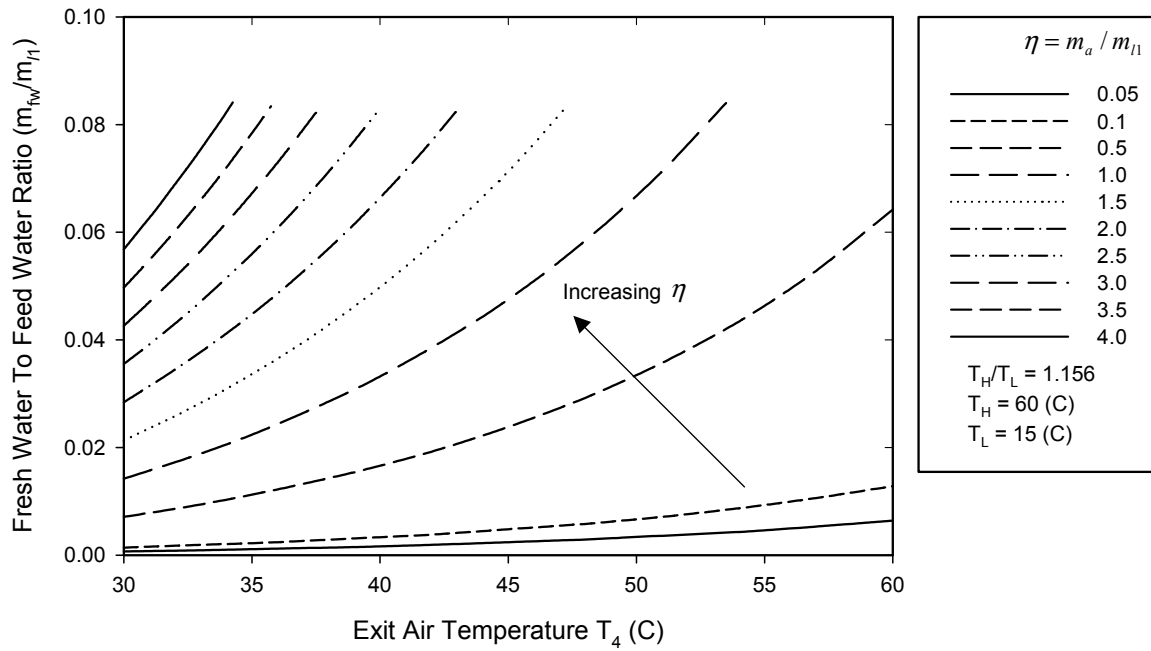


Figure 9 Fresh water production efficiency for $T_H=60^\circ\text{C}$.

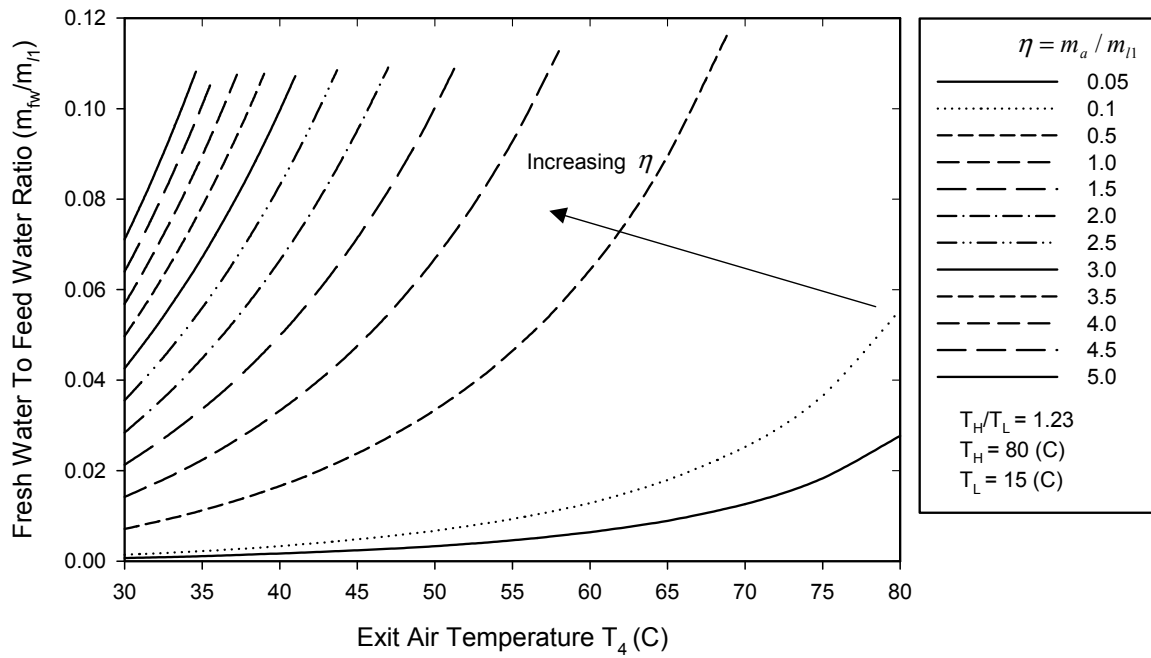


Figure 10 Fresh water production efficiency for $T_H=80^\circ\text{C}$.

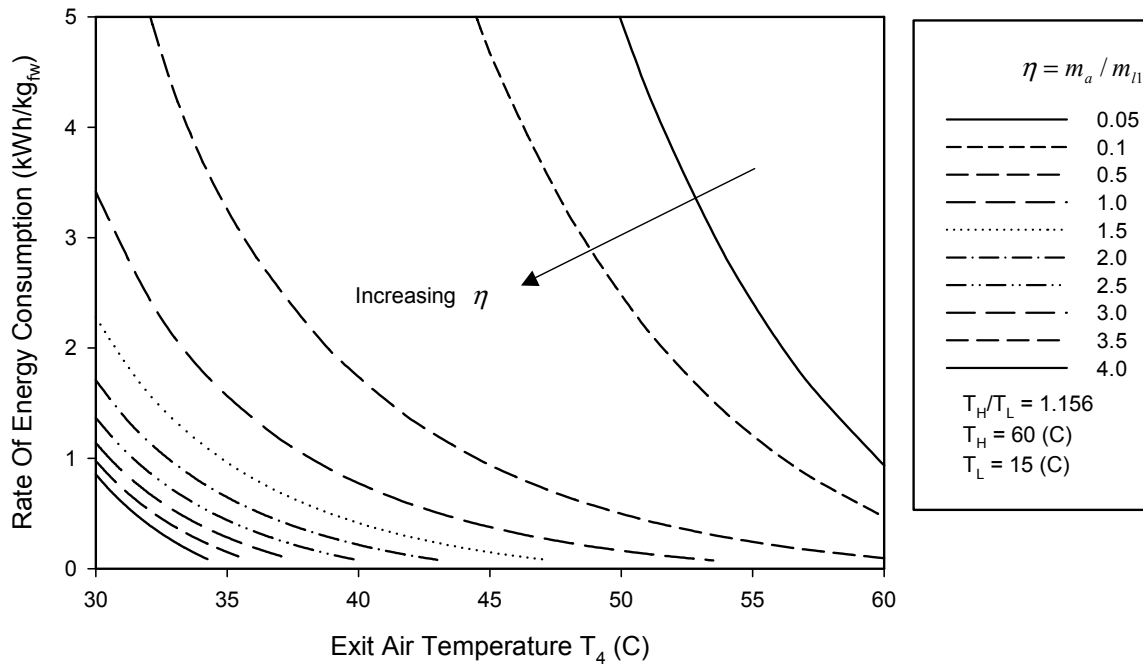


Figure 11 Rate of energy consumption for $T_H=60^\circ$ C.

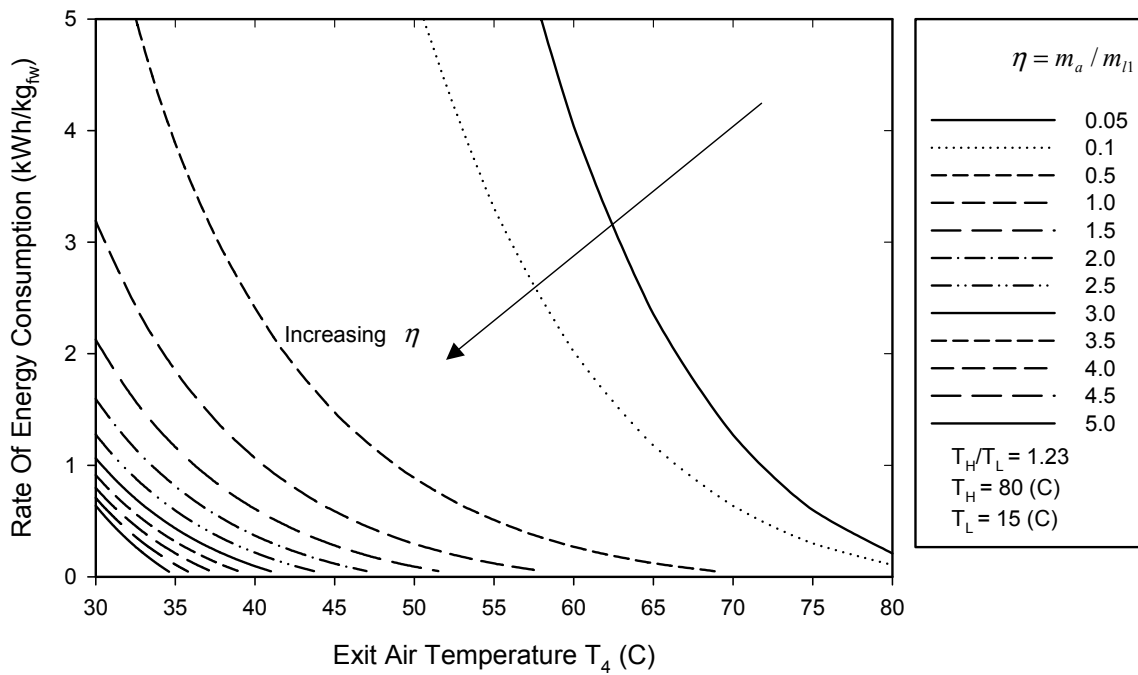


Figure 12 Rate of energy consumption for $T_H=80^\circ$ C.

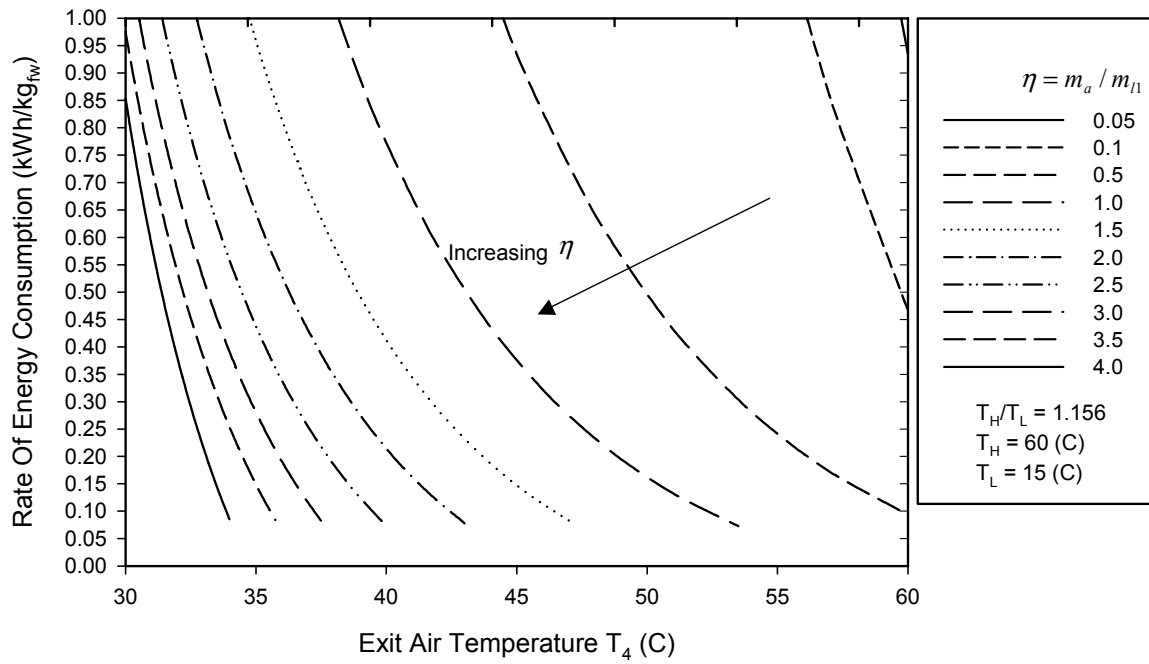


Figure 13 Rate of energy consumption on magnified scale for $T_H=60^\circ$ C.

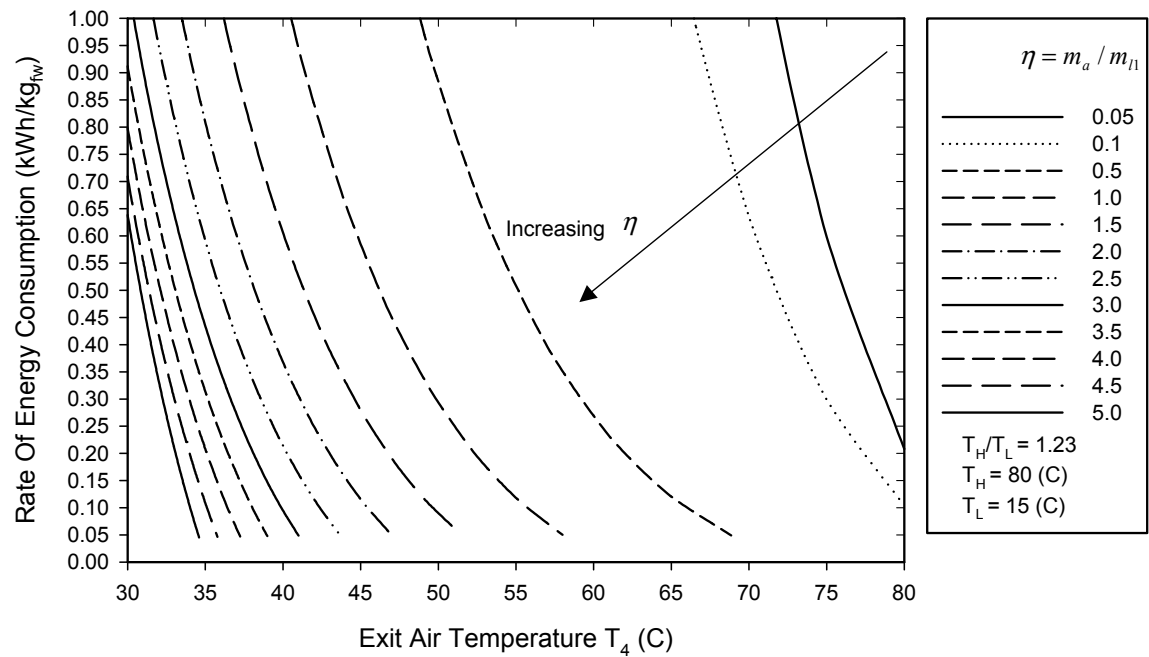


Figure 14 Rate of energy consumption on magnified scale for $T_H=80^\circ$ C.